



United States
Department of
Agriculture

Forest Service

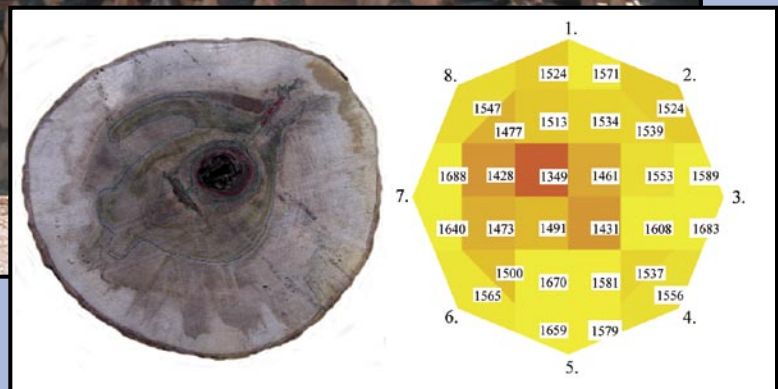
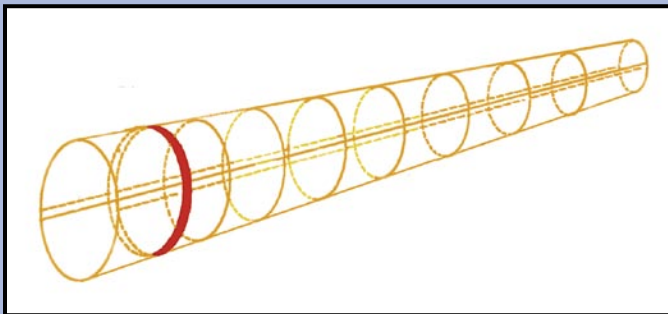
Forest
Products
Laboratory

General
Technical
Report
FPL-GTR-162



Nondestructive Evaluation of Incipient Decay in Hardwood Logs

Xiping Wang
Jan Wiedenbeck
Robert J. Ross
John W. Forsman
John R. Erickson
Crystal Pilon
Brian K. Brashaw



Abstract

Decay can cause significant damage to high-value hardwood timber. New nondestructive evaluation (NDE) technologies are urgently needed to effectively detect incipient decay in hardwood timber at the earliest possible stage. Currently, the primary means of inspecting timber relies on visual assessment criteria. When visual inspections are used exclusively, they provide no indication of the extent of internal deterioration that may exist in timber. In this study, time-of-flight, stress-wave tomography, and micro-drilling resistance methods were investigated for locating incipient decay in sugar maple logs. We found that the capability of the single-path time-of-flight method for decay detection is very limited, and the method can be used only to identify logs and trees with moderate and severe decay. Resistance-based detection of decay (including early stages) is effective if the resistance drilling device is oriented so that its path goes through the decay zone; however, orienting the drill through the decay is difficult to guarantee. A multi-sensor stress-wave device can overcome the path-dependent detection issue. Results from laboratory testing indicate that the eight-sensor two-dimensional stress-wave device has good potential for assisting in the detection of incipient decay in roundwood, such as logs and standing timber. However, to more effectively locate early-stage decay within a hardwood timber, more sensors should be added to the measurement system to obtain a higher resolution two-dimensional tomography image of a cross section. Field studies on standing hardwood timber should further investigate the effectiveness of

these NDE methods with improved systems and procedures. This research could benefit field foresters and managers in using NDE technologies to assess the health condition of hardwood timber in the forest and could potentially lead to significant economic savings.

Keywords: hardwood log, incipient decay, micro-drilling resistance, resistograph, stress wave, tomograph

Contents

	<i>Page</i>
Introduction.....	1
Technology Review	1
Time-of-Flight Stress-Wave Technique	1
Micro-Drilling Resistance.....	1
Stress-Wave Tomographic Imaging	2
Materials	2
Experimental Methods	3
Time-of-Flight Measurements	3
2D Stress-Wave Tomographic Imaging	4
Micro-Drilling Resistance.....	4
Deconstructive Assessment of Logs	4
Data Analysis	5
Results and Discussion	5
Single-Path Time-of-Flight Measurements.....	5
Stress-Wave Tomography	7
Micro-Drilling Resistance.....	7
Conclusions.....	8
Recommendations.....	8
Acknowledgments.....	9
References.....	9

November 2005

Wang, Xiping; Wiedenbeck, Jan; Ross, Robert J.; Forsman, John W.; Erickson, John R.; Pilon, Crystal; Brashaw, Brian K. 2005. Nondestructive evaluation of incipient decay in hardwood logs. Gen. Tech. Rep. FPL-GTR-162. Madison, WI: U.S. Department of Agriculture, Forest Service, Forest Products Laboratory. 11p.

A limited number of free copies of this publication are available to the public from the Forest Products Laboratory, One Gifford Pinchot Drive, Madison, WI 53726-2398. This publication is also available online at www.fpl.fs.fed.us. Laboratory publications are sent to hundreds of libraries in the United States and elsewhere.

The Forest Products Laboratory is maintained in cooperation with the University of Wisconsin. This article was written and prepared by U.S. Government employees on official time, and it is therefore in the public domain and not subject to copyright.

The use of trade or firm names in this publication is for reader information and does not imply endorsement by the United States Department of Agriculture (USDA) of any product or service.

The USDA prohibits discrimination in all its programs and activities on the basis of race, color, national origin, age, disability, and where applicable, sex, marital status, familial status, parental status, religion, sexual orientation, genetic information, political beliefs, reprisal, or because all or a part of an individual's income is derived from any public assistance program. (Not all prohibited bases apply to all programs.) Persons with disabilities who require alternative means for communication of program information (Braille, large print, audiotape, etc.) should contact USDA's TARGET Center at (202) 720-2600 (voice and TDD). To file a complaint of discrimination, write to USDA, Director, Office of Civil Rights, 1400 Independence Avenue, S.W., Washington, D.C. 20250-9410, or call (800) 795-3272 (voice) or (202) 720-6382 (TDD). USDA is an equal opportunity provider and employer.

Nondestructive Evaluation of Incipient Decay in Hardwood Logs

Xiping Wang, Research Associate

University of Minnesota–Duluth and Forest Products Laboratory, Madison, Wisconsin

Jan Wiedenbeck, Project Leader

USDA Forest Service, Northeastern Research Station, Princeton, West Virginia

Robert J. Ross, Project Leader

Forest Products Laboratory, Madison, Wisconsin

John W. Forsman, Assistant Research Scientist

John R. Erickson, Research Scientist

Michigan Technological University, Houghton, Michigan

Crystal Pilon, General Engineer

Forest Products Laboratory, Madison, Wisconsin

Brian K. Brashaw, Program Director

Natural Resources Research Institute, University of Minnesota–Duluth

Introduction

Decay can cause significant damage to high-value hardwood timber in the United States. Field foresters and managers are keenly interested in learning whether new nondestructive evaluation (NDE) technologies may be used to effectively detect incipient decay in standing hardwood timber at the earliest possible stage. Currently, the primary means of inspecting timber relies on visual assessment criteria. Whereas visual inspections are used extensively, they provide no indication of the extent of internal deterioration that may exist in timber. The objective of this study is to determine the effectiveness of several existing NDE technologies for locating incipient decay in standing hardwood timber. Results of this study will assist field foresters and managers in monitoring the health of the Nation's standing hardwood timber and identifying decay-infested trees in forests.

Technology Review

Time-of-Flight Stress-Wave Technique

Time-of-flight stress-wave technique has been successfully used in decay detection in a variety of wood structures (Pellerin and Ross 2002). The concept of detecting decay using this method is based on the idea that stress-wave propagation is sensitive to the presence of degradation in wood. In general terms, a stress wave travels faster through sound and high-quality wood than it does through deteriorated or low-quality wood. The time-of-flight of the stress wave is typically used as a predictor of the physical conditions inside the wood. By measuring the time-of-flight of a stress wave through a tree stem in the radial direction, the internal condition of the tree can be evaluated.

Time-of-flight of stress waves traveling perpendicular to the grain is affected by tree species. Mattheck and Bethge (1993) measured speed of sound in different species of healthy trees using a commercially available stress-wave timing unit. They found that speed variation exists both within species and between species. Generally, sound travels faster in hardwood species than in softwood species. For example, the speed of sound for healthy maple trees is from 1,000 to 1,600 m/s. However, for healthy Douglas-fir trees, it ranges from 900 to 1,300 m/s. For evaluating trees of different species, Divos and Szalai (2002) provided some baseline stress-wave velocities for intact healthy trees (Table 1).

Micro-Drilling Resistance

Micro-drilling resistance tools are being used increasingly in the field to characterize wood properties and detect abnormal physical conditions in structural timbers and

Table 1—Radial stress-wave velocities for intact trees (Divos and Szalai 2002)

Species	Radial stress-wave velocity (m/s)
Birch	1,140
Spruce	1,310
Silver fir	1,360
Japanese fir	1,450
Scotch pine	1,470
Black fir	1,480
Larch	1,490
Oak	1,620
Beech	1,670
Linden	1,690
Maple	1,690

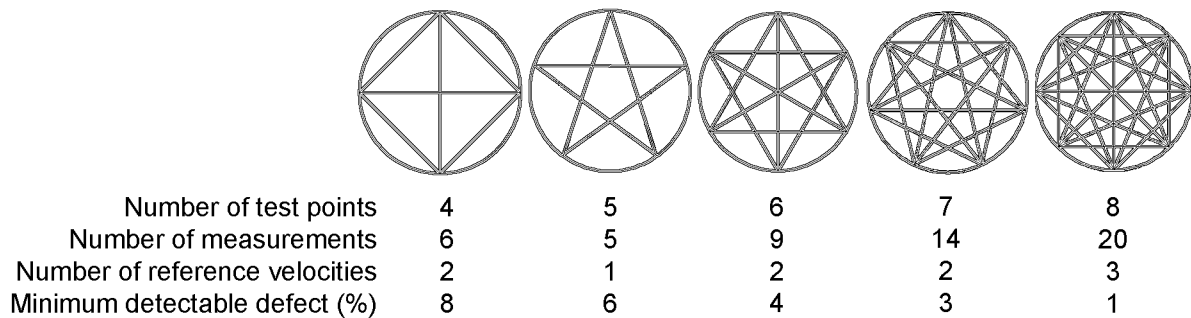


Figure 1—Sensor arrangements for multi-path time-of-flight measurements (Divos and Szalai 2002).

standing trees (Rinn 1994; Isik and Li 2003; Brashaw and others 2004, 2005). Our experience on tree quality assessment using the micro-drilling resistance tool also indicated that this technique could have good potential for detecting and defining the extent of incipient decay in softwood trees.

The micro-drilling resistance tool is a mechanical drill system that measures the relative resistance (drilling torque) of the material as a rotating drill bit is driven into the wood at a constant speed. It produces a chart showing the relative resistance profile for each drill path. Because it can reveal the relative density change along the drill path, it is typically used to diagnose the internal condition of structural timbers and urban trees.

The drill resistance R_D is defined as

$$R_D = \frac{T}{\omega} \quad (\text{Nm s/rad})$$

where T is drilling torque (Nm) and ω the angular speed (rad/s).

A micro-drilling resistance tool typically consists of a power drill unit, a small-diameter drill bit, a paper chart recorder, and an electronic device that can be connected to the serial interface input of any standard personal computer. The diameter of the drill bit is typically very small, from 2 to 5 mm, so that any weakening effect of the drill hole on the wood cross section is negligible.

Stress-Wave Tomographic Imaging

The sensitivity of the time-of-flight stress-wave technique is limited. A single-pass stress-wave measurement can only detect internal decay that occupies 20% or more of the total cross-section area (Ross and others 2004). To increase the reliability of the inspection and define the extent and location of any internal decay, it would be practical to conduct multiple measurements in different orientations at one cross section, especially for suspect trees. Tomographic inversion of stress-wave data from multiple measurements could allow inspectors to obtain an image of the distribution of stress-wave transmission times in the cross section and help define the extent and location of internal decay with accuracy.

Stress-wave tomography is an NDE technique that refers to the cross-sectional imaging of an object from data collected by measuring the stress-wave properties from multiple directions in a plane. Different types of stress waves can be used, but the most convenient are bulk longitudinal waves. Tomographic images can be constructed from many stress-wave parameters, such as time-of-flight, amplitude, frequency spectrum, and phase. The three main types of algorithms that can be used to form tomographic images from stress-wave data are transform techniques, iterative techniques, and direct inversion techniques (Bucur 2002, 2005).

Divos and Szalai (2002) proposed several possible stress-wave measurement arrangements with testing points ranging from four to eight (Fig. 1). The minimum detectable defect size can be theoretically determined, assuming that the defect approximates a circle. As indicated in Figure 1, the minimum detectable defect sizes are 8%, 6%, 4%, 3%, and 1% of the cross-section area for 4, 5, 6, 7, and 8 test points arrangements, respectively. The reference velocity determination is a key step in constructing tomographic images. The reference velocity is defined as the velocity in the healthy wood of a tree. Because stress-wave velocity depends on anatomical directions, two or more reference values may be needed, depending on the measurement arrangement.

Materials

Twelve freshly cut sugar maple (*Acer saccharum*) logs representing a range of discoloration and decay were hand-picked at a local mill in Houghton, Michigan. The selection process segregated four classes of logs: three logs with no decay (control group), three logs with severe discoloration (light decay), three with small to medium levels of decay, and three with medium to severe levels of decay. No logs had decay along their full length, thereby permitting comparisons between sound and decayed wood both within classes and within the same log. Logs were then shipped to the USDA Forest Products Laboratory (FPL) in Madison, Wisconsin, where various NDE testing procedures were performed.

Table 2—Diameters and length of sugar maple logs tested

Log no.	Log diameter (cm (in.))				Length (cm (in.))	
	Butt end		Small end			
1	35.5	(14.0)	28.8	(11.3)	265.4	(104.5)
2	43.0	(16.9)	36.5	(14.4)	266.7	(105.0)
3	29.8	(11.7)	27.5	(10.8)	266.7	(105.0)
4	37.8	(14.9)	37.3	(14.7)	266.7	(105.0)
5	41.0	(16.1)	40.5	(15.9)	257.2	(101.3)
6	32.4	(12.8)	28.0	(11.0)	259.1	(102.0)
7	42.1	(16.6)	34.7	(13.7)	268.6	(105.8)
8	40.3	(15.8)	34.8	(13.7)	270.5	(106.5)
9	26.1	(10.3)	25.8	(10.1)	254.0	(100.0)
10	36.0	(14.2)	33.3	(13.1)	264.2	(104.0)
11	29.5	(11.6)	31.8	(12.5)	266.7	(105.0)
12	36.8	(14.5)	34.4	(13.5)	266.7	(105.0)

Experimental Methods

The logs were randomly numbered and the ends were marked with paint when they arrived at FPL. To document the general physical characteristics of the log samples, we first measured the diameters (butt end and small end) and length of each log. Table 2 shows the diameters and length of 12 sugar maple logs. The log samples were all about 2.64 m (104 in.) long. The butt-end diameter ranged from 26.1 to 43.0 cm (10.3 to 16.9 in.), and the small-end diameter ranged from 25.8 to 40.5 cm (10.1 to 15.9 in.).

In this study, three promising NDE techniques were evaluated for detecting internal incipient decay of sugar maple logs. The instrumentation systems employed included the Fakopp (Fakopp Enterprise, Agfalva, Hungary) Microsecond Timer (time-of-flight stress-wave measurement), Fakopp

2D multi-channel microsecond timer (stress-wave-based tomograph), and the IML-RESI F400 (Instrument Mechanic Labor, Inc., Kennesaw, Georgia) measuring instrument (micro-drilling resistance). We originally planned to examine the use of an ultrasound device (Sylvatest Duo, Concept Bois Structure, Les Ecorces, France); however, exploratory tests with this ultrasound equipment showed a serious coupling problem between the probes and the rough surface of the logs. The ultrasound waves seemed unable to transmit properly through the log cross section without having the bark removed. Considering the limited testing time available and probable adaptation issues in the field, we decided to eliminate the use of Sylvatest Duo from our experimental procedure.

Figure 2 outlines measurement locations and the scan path along the length of a log. Because the decay detection mechanisms of all three techniques examined are limited to provide one- or two-dimensional information only, multi-plane measurements on the logs are necessary for accurate assessment. Therefore, each log was properly oriented and tested in two main directions (a-a, horizontal; and b-b, vertical) and at multiple locations along the length. The butt end of each log was more intensively scanned (15.2 cm (6 in.) apart) because decay often occurs at the lower part of a tree. The remaining NDE measurements were taken along the length of the log with less intensity (30.5 cm (12 in.) apart).

Time-of-Flight Measurements

To facilitate testing, each log was supported by two concrete blocks, one on each end, 0.9 m (3 ft) above the ground. After the log was properly oriented and secured, the upper surface of the log was marked using a chalk-line according to the testing diagram (Fig. 2). Time-of-flight measurements

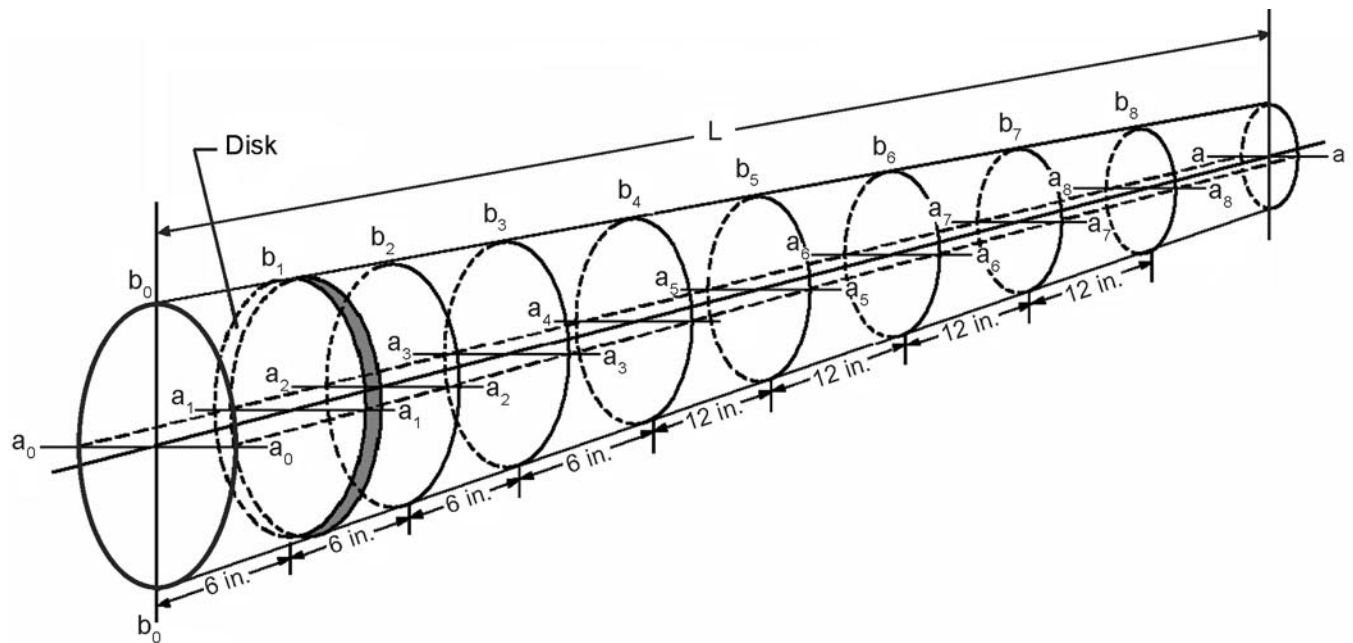


Figure 2—Measurement locations and scan path along the length of a log.

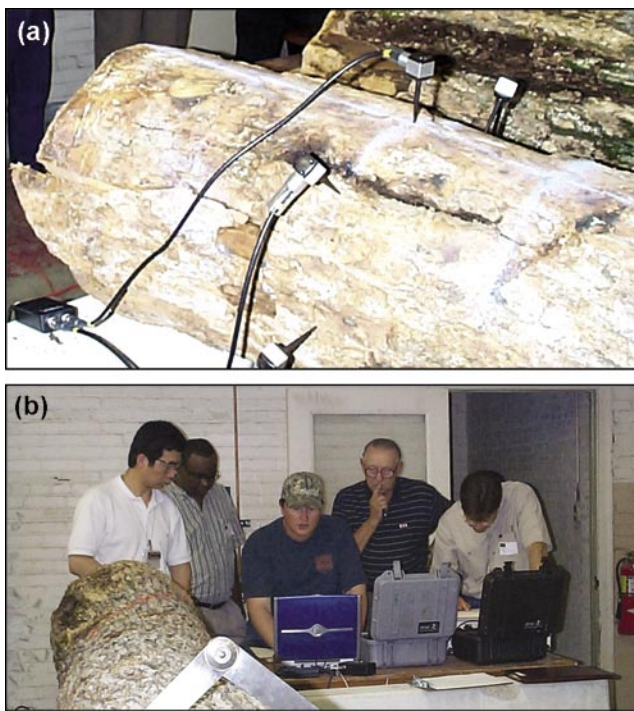


Figure 3—Multi-channel stress-wave measurement system: (a) Placement of transducers, (b) measurement and recording equipment.

were conducted using a Fakopp Microsecond Timer in both horizontal (a–a) and vertical (b–b) directions at each scan location.

The timer is composed of two needles (with a transducer built in to each needle) and a time-of-flight display unit. For each measurement, two needles were inserted into the log surface through the bark and aligned in a transverse path across the center of the log. Care was taken to locate transducer probes away from obvious surface defects. The needles were connected to the timer unit. A stress wave was initiated through a hammer tap on the start transducer's back impact surface. The timer displayed the travel time of the stress wave between two transducers.

2D Stress-Wave Tomographic Imaging

We used an eight-channel stress-wave device (Fakopp 2D Microsecond Timer) to collect time-of-flight data from each test plane in the logs. Figure 3 shows the use of the multi-channel stress-wave measurement system in testing a log sample.

The tomographic measurements were conducted at multiple locations for each log sample (Fig. 2). At each test location, the diameters of the long axis and short axis and the circumference of the cross section were measured using a caliper and a tape measure. This information was used as an input for the system software to map the approximate geometric form of the cross section and determine the location of each transducer around the circumference. Eight transducers were



Figure 4—Micro-drilling resistance test.

then mounted onto the log following the sensor arrangement specified by the software. We carefully inserted the needle probes properly into the sapwood by penetrating the bark to eliminate the signal disturbance from bark. The transducers were then tapped one by one using a hammer, and following each tapping, an array of time-of-flight data were collected through a data acquisition system. A complete data matrix was obtained through this measurement process at each location and saved for further tomographic image analysis.

Micro-Drilling Resistance

We tested log samples with the IML-RESI F400 measuring instrument (Fig. 4). The original plan for micro-drill tests on each log sample was to obtain resistance profiles in both horizontal (a–a) and vertical (b–b) directions (Fig. 2) and at each scan location along the length of the log. This procedure would provide a quasi-three-dimensional resistance profile for each log sample tested and therefore allow for more accurate assessment of internal decay conditions. However, this procedure was not carried out during log testing because of time limitations. The testing procedure was modified to test in the horizontal direction only and at selected scan locations.

As the drill bit entered and passed through the wood, the relative resistance, which is determined by the drilling torque R_D and angular speed ω , was recorded on a wax paper graph and stored in an electronic unit. Each resistance chart was properly coded to track its drilling location along the length of the log. The electronic files were transmitted to a computer after testing for further analysis. The maximum drilling depth of the tool we used is 400 mm, which is long enough to penetrate the whole cross section for most samples we tested. For the few logs with diameters slightly greater than 400 mm, the resistance information obtained from this tool is considered good enough to reveal the internal physical condition of the cross section.

Destructive Assessment of Logs

After NDE measurements were completed, a 3.8- to 5-cm- (1.5- to 2-in.-) thick disk was cut from each measurement location. Ten disks were obtained from each log. Each disk was then carefully surfaced and physically examined for

Table 3—Radial stress-wave velocities for intact sections of sugar maple logs

Log no.	Radial stress-wave velocity (m/s)			Condition	Number of sound disk sections
	Mean	Min	Max		
1	1329	1182	1611	Intact sections	7–9
2	—	—	—	Decayed	No sound sections
3	1599	1419	1667	Intact sections	1, 3, 5, 7
4	—	—	—	Decayed	No sound sections
5	1436	1329	1564	Intact sections	6–10
6	1705	1562	1843	Intact	All sections sound
7	1737	1691	1804	Intact sections	8, 9, 10
8	1713	1548	1840	Intact sections	5, 9
9	1680	1535	1794	Intact sections	1–6, 8, 9
10	1844	1761	1963	Intact sections	5, 9
11	1616	1520	1707	Intact sections	1–7, 9
12	—	—	—	Decayed	No sound sections

internal conditions in terms of the discoloration and the level and location of decay. A digital picture was taken of the cross section of each disk, and the disks were mapped into different quality regions using different color lines. The color codes for mapping disks are as follows:

- Blue/Purple* – stain (dark, deep discoloration);
- Green* – incipient decay (soft wood with open pores but hard to mark with fingernails);
- Red* – decay (super soft wood but still in place); and
- Black* – hole (missing wood, complete or partial).

All disk samples were weighed after they were cut from the logs. Oven-dry weights for one disk from each log were to be collected but because of the rapid rate of bacterial or fungal infection and time-to-ship slowdowns, these weights were not obtained.

Data Analysis

The general approach of data analysis is to compare data from all three techniques with real images of the log cross sections and determine if various NDE measures have significant relationships with the levels of decay in sugar maple logs. The specific predictive parameters considered for decay detection includes time-of-flight (TOF), relative velocity drop (RVD), and relative drill resistance (R_D).

For time-of-flight measurement, the transmission time data were converted into velocity values (m/s) using

$$V_i = \frac{D_i}{TOF_i}$$

where V_i is stress-wave velocity (m/s), D_i is the diameter (or distance between two sensors) in the radial path, and TOF_i is the transmission time in the radial path.

To make a direct comparison on time-of-flight measurement, the stress-wave velocity was mapped along the length of each log. We made a statistical comparison of stress-wave velocity between log classes (control and different decay levels) and the healthy and decayed sections within a log.

We used stress-wave data from multiple-path measurements to construct two-dimensional tomograph images with a cell-based backprojection program (Fakopp Backprojection V 1.5). The tomograph image shows the distribution of acoustic velocity in a cross section and identifies the location and extent of internal decay.

Results and Discussion

Single-Path Time-of-Flight Measurements

Radial stress-wave velocities in two perpendicular directions were mapped along the length of each log. The velocity in each direction was evaluated individually to maximize the chance of detecting any decay that may exist at each cross section. The key to interpreting these results is to determine the appropriate reference velocity based on the measurements of intact logs or the intact section of a log. Among 12 log samples, three logs (log 2, 4, and 12) were identified as having incipient and moderate decay through the whole length. Log 6 was entirely intact. Most log samples have localized decay in some sections. Table 3 shows the stress-wave velocity values for all intact (sound) logs or sections of logs.

It appears that the radial stress-wave velocity data of intact sugar maple logs have a large variability, ranging from 1,182 to 1,963 m/s. Even the average velocity of each log or section ranges from 1,329 to 1,844 m/s. This variation is likely caused by local property difference in logs. The average velocity of sugar maple logs is 1,629 m/s, which is very close to the value given by Divos and Szalai (2002) (Table 1).

Because of the large variation in radial stress-wave velocity measurements in intact logs, it is difficult to determine a velocity benchmark for field-data interpretation. This will greatly impair the use of time-of-flight techniques for detecting internal decay in logs and trees, especially for detecting decay at the early stages. However, to detect moderate and severe decay in logs or trees, three choices are seemingly available for determining a reference velocity for the

Table 4—Decay assessment based on time-of-flight measurements ($V_{ref I} = 1,182$ m/s)

Log no.	Cross sections of log									
	1	2	3	4	5	6	7	8	9	10
1	***	***		*	***	***	-	-	-	*
2	**		*		-	-		*	*	***
3	-		-		-		-		-	-
4	*	-	-	-	-	-	-	-	-	-
5	*	-	-	*	-	-	-	-	-	-
6	-									
7	-									
8	-									
9	-									
10	-									
11	-									
12	-									

Table 5—Decay assessment based on time-of-flight measurements ($V_{ref II} = 1,329$ m/s)

Log no.	Cross sections of log									
	1	2	3	4	5	6	7	8	9	10
1	***	***		*	***	***	**	*	**	*
2	**		*		-	-		*	**	***
3	-		-		-		-		-	-
4	*	*	-	-	-	-	-	-	-	-
5	**	**	-	*	-	-	-	*	-	-
6	-									
7	-									
8	*	-	-	-	-	-	-	-	-	-
9	-									*
10	-									-
11	-									-
12	-									-

Table 6—Decay assessment based on time-of-flight measurements ($V_{ref III} = 1,629$ m/s)

Log no.	Cross sections of log									
	1	2	3	4	5	6	7	8	9	10
1	***	***		**	***	***	**	**	**	**
2	**		**		**	**		**	**	***
3	*		*		**		*		*	**
4	**	**	**	**	**	**	**	**	*	*
5	**	**	**	**	**	**	**	**	**	**
6	-		-		-		-		**	*
7	-		-		-	**	*	-	-	-
8	**	**	-	*	-	-	-	-	*	**
9	-		*	-	-	-	-	*	*	**
10	-		-		-		-	-	-	-
11	**		**	**	*	-	**	*	*	-
12	-		-	*	-	-	*	*	**	**

species: (1) using the minimum value of all intact velocity data ($V_{ref I} = 1,182$ m/s); (2) using the minimum value of average velocity of individual logs ($V_{ref II} = 1,329$ m/s); and (3) using an average value from all intact velocity data ($V_{ref III} = 1,629$ m/s).

Tables 4 to 6 show interpretation of time-of-flight measurements based on three reference velocities. Each cell represents one cross section in a log that was tested. In addition

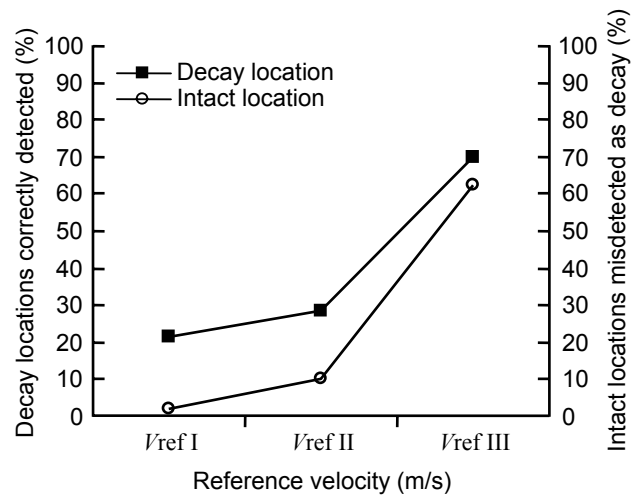


Figure 5—Decay locations correctly detected and intact locations misidentified in relation to reference velocities. $V_{ref I}$, minimum value of radial velocity of intact logs, $V_{ref II}$, minimum value of average velocity of individual logs; $V_{ref III}$, average of all intact velocity.

to using three reference velocities as different strategies to separate solid logs and decayed or suspect logs, a radial velocity of 1,000 m/s is used as a general reference (V_0) to detect severely decayed logs. This general reference velocity was based on the observation that log sections with stress-wave velocities of less than 1,000 m/s all had severe decay or holes in the cross section.

The cells in Tables 4 to 6 were rated into four categories by comparing the measured radial stress-wave velocity with the reference velocities:

- (1) Solid—radial velocities in two perpendicular directions are both higher than the reference velocity, marked as “-”;
- (2) Suspect—radial velocity in one of the directions is lower than the reference velocity, marked as “*”;
- (3) Decay—radial velocities in two directions are lower than the reference velocity, marked as “***”;
- (4) Severe decay—radial velocity in one of the directions is lower than the general reference velocity (1000 m/s), marked as “***”.

Because the reference velocity was ambiguous, no attempt was made to further evaluate the severity of the decay once the inspection location was determined to be decayed or suspect on the basis of the reference velocity.

Based on the assessment of all disks cut from the log samples, 60 locations were confirmed to have localized decay, and 48 locations were confirmed as intact. The interpretation based on reference velocities was then compared with this destructive assessment. Figure 5 shows the effectiveness of different decay detection strategies. Interpretation based on $V_{ref I}$ (minimum value of radial velocity of intact logs) had the lowest decay detection rate (21.7%) on decay locations but also has the lowest misdetection rate (i.e., false

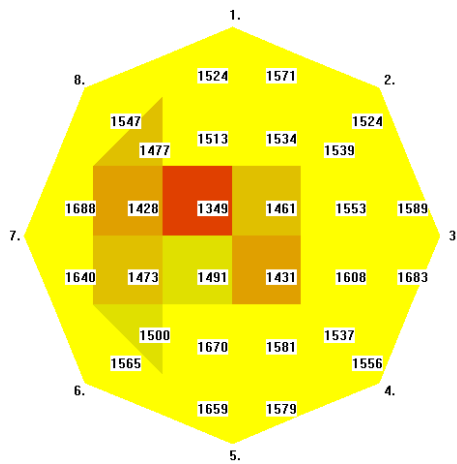


Figure 6—Example of a tomographic image matching well with the decay area. (The line mark on the disk photo corresponds to point 1 in the tomographic image.)

positives) on intact locations. Interpretation based on $V_{ref III}$ (average of all intact velocity) gave the highest decay detection rate (70%), but the misdetection rate on intact locations is also the highest (62.5%). The implication is that the capability of single-path time-of-flight method for decay detection is very limited and can only be used to identify logs and trees with a significant amount of decay, such as logs 1 and 2.

Stress-Wave Tomography

Stress-wave propagation in wood is, by its nature, determined by the anisotropic behavior of wood. This means that stress waves travel at different velocities in different anatomical directions. As such, the construction of tomographic images from multi-path time-of-flight measurements would require multiple reference velocities, such as radial reference velocity, tangential reference velocity, and near-tangential or near-radial reference velocity. The back-projection software we used for constructing tomographic images was designed to determine the reference velocities automatically for each test location. Therefore, the two-dimensional image can be formed from stress-wave data based on self-calibrated reference velocities.

The evaluation process is based on the comparison between measured velocities and the reference velocities. The line where the measured velocity is lower than the reference velocity by a certain percentage (this information is unknown to users) is marked as the “defect line.” The intersection of two defect lines designates the defect location, which is marked as a red area. Results from sugar maple logs show that the projected decay images and actual decay areas overlap fairly accurately in many cases. Figure 6 demonstrates an example of a two-dimensional tomographic image obtained from log testing alongside the real image of the corresponding disk. The decay areas marked by red lines on the disk are well reflected on the tomographic image. However, in many other cases, the projection is not very successful,

with the images either not matching the real decay areas well (Figure 7a), failing to show a decay area (Figure 7b), or showing a solid area as having decay or suspect zone (Figure 7c).

To determine the overall accuracy of the stress-wave tomography technique in detecting various degrees of decay in sugar maple logs, each tomographic image was compared with its corresponding real disk image and rated in a qualitative manner: – represents no decay; + represents incipient decay; ++ represents moderate decay; and +++ represents severe decay or large void.

Table 7 shows the decay assessment results based on real disk images, and Table 8 shows the evaluation results based on tomographic images. Each cell in the tables represents one test location in a specific log. On the basis of the rating analysis, about 62% of the decay locations were detected, and 8.5% of the intact locations were misidentified as suspect or decayed.

Overall, accuracy of the eight-channel tomographic imaging technique is much higher than that of the single-path time-of-flight technique, but the precision of image projection needs to be improved to successfully detect incipient decay of hardwood timber in the field.

Micro-Drilling Resistance

Micro-drilling resistance tests on log samples were performed at the same locations where single-path and multi-path time-of-flight measurements were made, but only in one orientation. Each resistance chart represents one drilling at a specific location and in a horizontal radial direction (along the a axis shown in Fig. 2). The amplitude in the vertical axis indicates the relative resistance of the wood (in percentage) in relation to the drilling depth along the radial direction.

Figure 8 shows three resistance profiles and the radial stress-wave velocity map for log 1. Based on single-path

Table 7—Decay assessment based on disk images

Log no.	Cross sections of the log									
	1	2	3	4	5	6	7	8	9	10
1	++	++	++	++	+++	+	-	-	-	+
2	++		+		+	+		+	++	+
3	-		-		-		-		+	+
4	++	++	++	++	++	++	+	+	+	+
5	+	+	+	+	+	-	-	-	-	-
6	-		-		-		-		-	-
7	++	++	++	++	++	+	++	-	-	-
8	++	++	+	+	-	-	-	-	-	+
9	-	-	-	-	-	-	+	-	-	+
10	+	+	+	+	-	-	-	-	-	
11	-	-	-	-	-	-	-	+	-	++
12	+	+	+	+	+	+	++	++	++	++

Table 8—Decay assessment based on tomographic images

Log no.	Cross sections of the log									
	1	2	3	4	5	6	7	8	9	10
1	++	++	++	++	+++	++	-	-	-	+
2	++		+		-	-		+	++	++
3	-		-		-		-		-	-
4	++	+	-	-	-	-	+	-	-	+
5	++	++	++	+	+	-	-	-	-	-
6	-		-		-		-		-	-
7	-	-	-	-	-	-	+	-	-	-
8	+	-	+	-	-	+	-	-	+	+
9	-	-	-	-	-	+	+	-	-	-
10	-	+	-	+	-	-	-	-	-	
11	-	-	-	++	-	-	-	+	-	++
12	+	+	+	+	-	-	+	+	+	+

time-of-flight measurements, locations 1, 2, 5, and 6 have been identified as decay areas because these sections recorded radial velocities less than 1000 m/s. The resistance profiles of location 2 and 5 both confirmed this assessment, showing a relative resistance drop at the center of their profiles. Using resistance charts, the location and extent of decay can also be easily determined. In contrast to the effect of decay on relative resistance, Figure 8d demonstrates the resistance profile of an intact section, with no sudden resistance drop or flat trace recorded.

Results indicate that the micro-drilling resistance test is effective in detecting and defining the extent of internal decay, including early stages of decay, if the resistance drilling device is oriented so that its path goes through the decay zone. However, orienting the drill through the decay is difficult to guarantee. Figure 9 shows the effect of the drilling path on the result. With the drilling path in line with the decay zone, decay was properly detected and reflected on the resistance profile (Figure 9a). When the drilling path was only slightly away from the decay zone (Figure 9b), the decay was undetected. Considering the orientation limitation,

the micro-drilling resistance method is best used to confirm and determine the extent of decay in hardwood timbers after decay or suspect areas are detected by other techniques.

Conclusions

Twelve freshly cut sugar maple (*Acer saccharum*) logs with various decay levels were examined using three nondestructive evaluation (NDE) techniques including time-of-flight, stress-wave tomography, and micro-drilling resistance methods. The capability and accuracy of each technique for detecting internal decay in the logs were determined by comparing the NDE measurement data with destructive assessment results from disks cut from the logs. Based on the observation and data analysis results, we conclude the following:

1. The capability of the single-path time-of-flight method for incipient decay detection in sugar maple logs is limited because radial stress-wave velocity varies substantially for intact logs, and a standard reference velocity for data interpretation is not readily available. This technique could be used to identify logs and trees that have moderate and severe internal decay.
2. The results indicate that micro-drilling resistance is effective in detecting and defining the extent of internal decay, including early stages of decay, if the resistance drilling device is oriented so that its path goes through the decay zone. However, orienting the drill through the decay is difficult to guarantee. Considering the orientation limitation, the micro-drilling resistance method should be limited to confirm and determine the extent of decay in hardwood timbers after decay or suspect areas are detected by other techniques.
3. Compared to the single-path time-of-flight measurement, the stress-wave tomography technique, based on multi-path time-of-flight measurements, has good potential for detecting incipient decay in roundwood, such as logs and standing timber. For more effectively locating early-stage decay within hardwood timber, however, improvements need to be made in both the measurement system and the back-projection program to obtain a higher resolution 2D tomography image of a cross section.

Recommendations

With a better understanding of the capability and limitations of three NDE methods, future studies should focus on improving the measurement quality and increasing the accuracy of decay detection for the multi-path stress-wave tomograph method. An in-depth investigation of velocity distribution patterns in intact and decayed log cross sections for different species should be conducted, and appropriate reference velocities should be determined and used to replace the default values in the current image projection program.

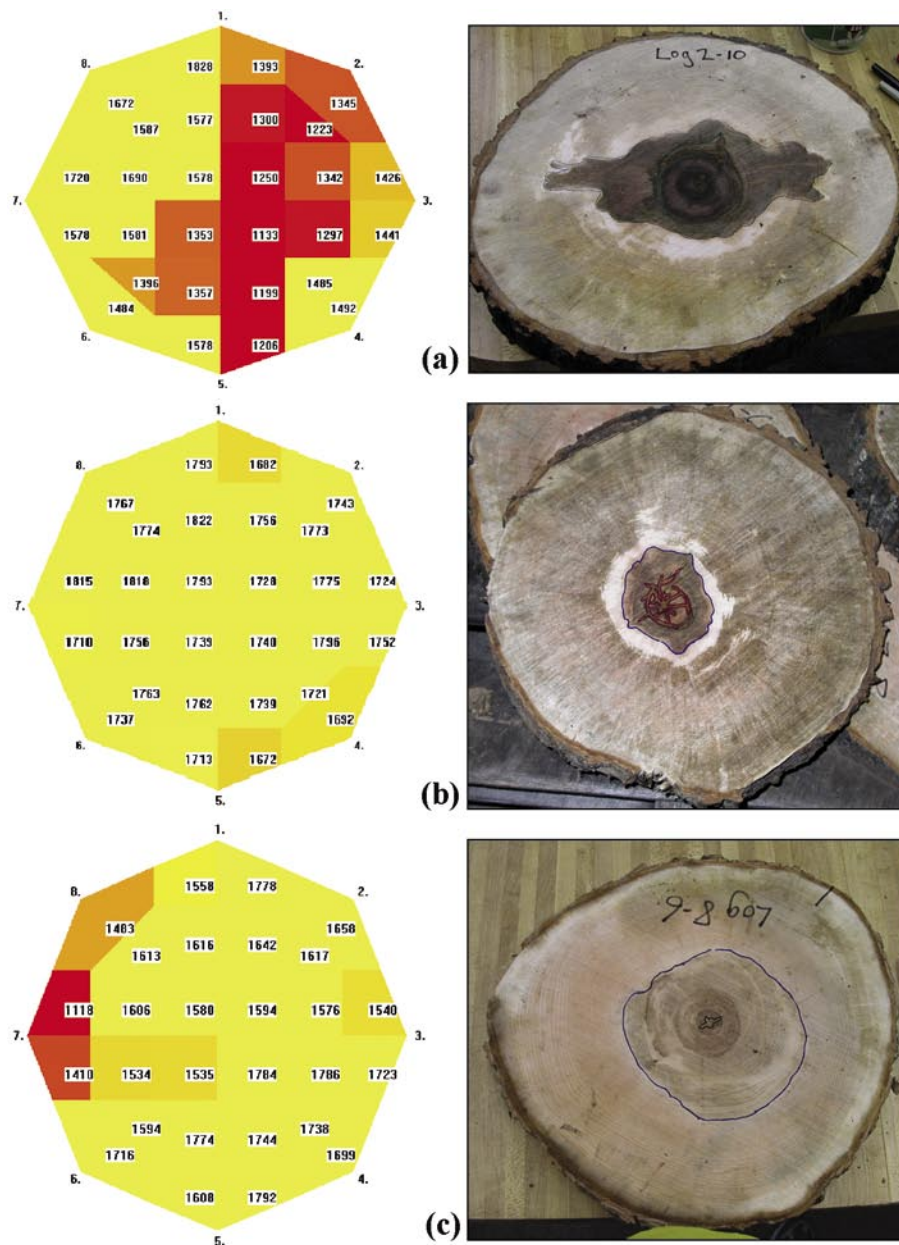


Figure 7—Examples of unsuccessful tomographic images. (a) Tomographic image does not match well with the decay area. (b) Tomographic image failed to identify incipient decay in the center. (c) Tomographic image misidentified a solid area as a decay zone.

Acknowledgments

This project was funded through a cooperative research agreement between the Natural Resources Research Institute of the University of Minnesota–Duluth; Michigan Technological University; USDA Forest Service Northeastern Research Station; and Forest Products Laboratory. We greatly appreciate the assistance of Dr. Ben Dawson-Andoh and Jeff Slahor of West Virginia State University during testing.

References

Brashaw, B.K.; Vatalaro, Robert J.; Erickson, John R.; Forsman, John W.; Ross, Robert J. 2004. A study of technologies to locate decayed timber bridge members. Final report, NRRI/TR–2004–06, Natural Resources Research Institute, University of Minnesota–Duluth, Duluth, MN. Prepared for USDA Forest Products Laboratory.

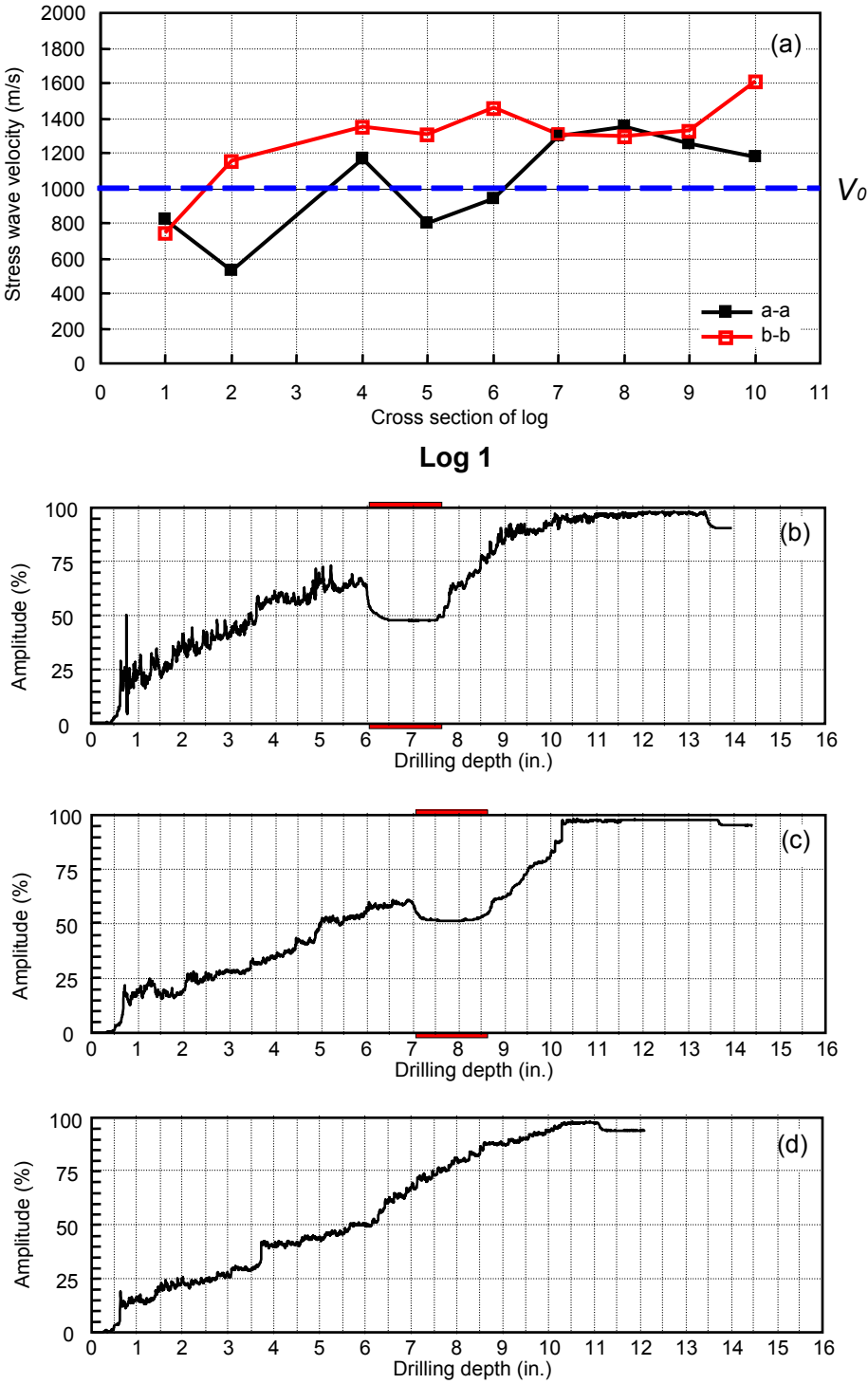


Figure 8—Stress-wave velocity map of log 1 and the relative resistance profiles at three different locations (section 2, 5, and 8). (a) Map of radial stress-wave velocity. (b) Resistance profile of section 2. (c) Resistance profile of section 5. (d) Resistance profile of section 8.

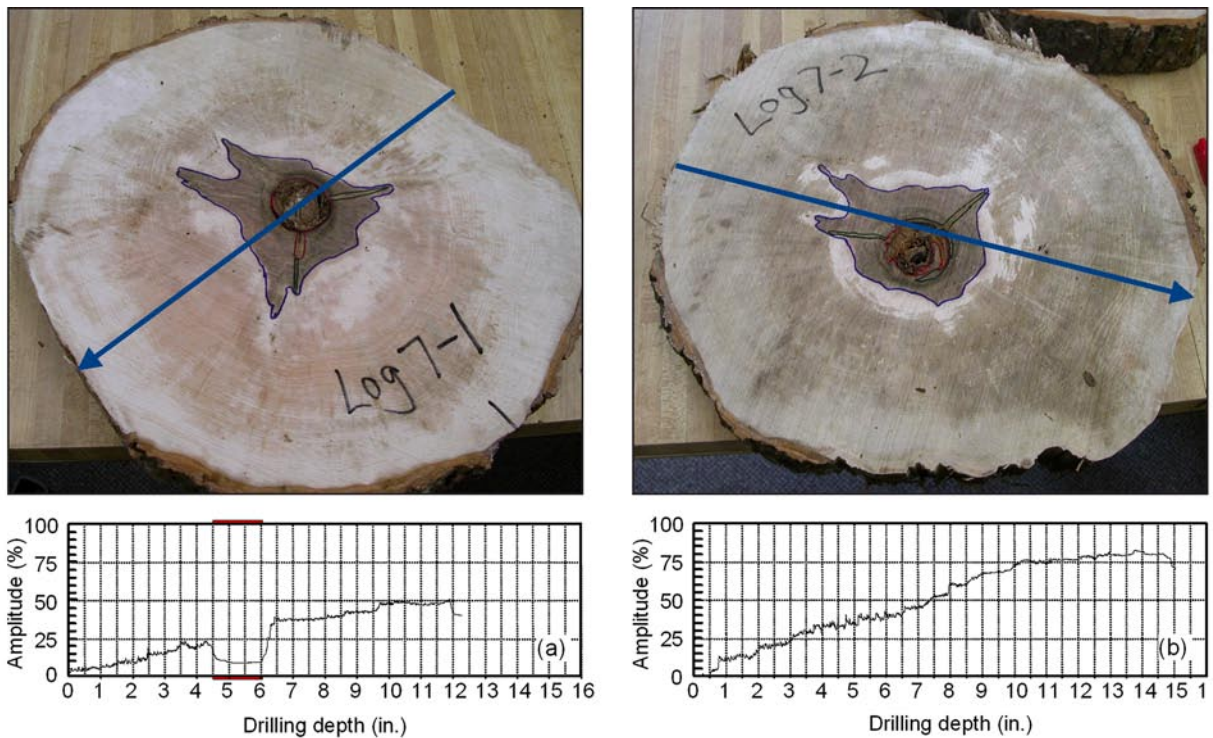


Figure 9—Orientation of drilling path and decay zone within a cross section: (a) Drilling path in line with the decay zone, (b) drilling path not in line with the decay zone.

Brashaw, Brian K.; Vtalaro, Robert J.; Wacker, James P.; Ross, Robert J. 2005. Condition assessment of timber bridges: 1: Evaluation of a micro-drilling resistance tool. Gen. Tech. Rep. FPL-GTR-159. Madison, WI: U.S. Department of Agriculture, Forest Service, Forest Products Laboratory. 8 p.

Bucur, Voichita. 2005. Ultrasonic techniques for nondestructive testing of standing trees. *Ultrasonics* 43 (2005) 237–239.

Bucur, Voichita. 2002. High resolution imaging of wood. In: *Proceedings of the 13th International Symposium on Non-destructive Testing of Wood*. August 19–21, 2002. Berkeley, CA: 231–236.

Divos, Ferenc; Szalai, L. 2002. Tree evaluation by acoustic tomography. In: *Proceedings of the 13th International Symposium on Nondestructive Testing of Wood*. August 19–21, 2002. Berkeley, CA: 251–256.

Isik, Fikret; Li, Bailian. 2003. Rapid assessment of wood density of live trees using the Resistograph for selection in tree improvement programs. *Can. J. For. Res.* 33: 2426–2435.

Mattheck, C.G.; Bethge, K.A. 1993. Detection of decay in trees with the Metriguard Stress Wave Timer. *Journal of Abriculture*. 19(6): 374–378.

Pellerin, R.F.; Ross, R.J. 2002. *Nondestructive testing of wood*. Madison, WI: Forest Products Society. 210 p.

Rinn, Frank. 1994. Catalog of relative density profiles of trees, poles, and timber derived from resistograph micro-drilling. In: *Proceedings of the 9th International Symposium on Nondestructive Testing of Wood*. September 22–24, 1993. Madison, WI. Published by Conferences & Institutes, Washington State University. 1994. pp. 61–67.

Ross, R.J., Brashaw, B.K.; Wang, X.; White, R.; Pellerin, R.F. 2004. *Wood and Timber Condition Assessment Manual*. Forest Products Society, Madison, WI.

Wang, Xiping; Divos, Ferenc; Pilon, Crystal; Brashaw, Brian K.; Ross, Robert J.; Pellerin, Roy F. 2004. Assessment of decay in standing timber using stress wave timing nondestructive evaluation tools—A guide for use and interpretation. Gen. Tech. Rep. FPL-GTR-147. Madison, WI: U.S. Department of Agriculture, Forest Service, Forest Products Laboratory. 12 p.

